JOURNAL OF MATERIALS SCIENCE 23 (1988) 481–487

The fabrication of O′-sialon ceramics by pressureless sintering

M. B. TRIGG*, K. H. JACK
The Wolfson Research Group for High-Strength Materials,
The University of Newcastle upon Tyne, Newcastle upon Tyne NE1 7RU, UK

Low-porosity ceramics with O′-sialon as the major crystalline phase have been successfully fabricated by pressureless sintering. Densification at 1400 to 1800° C is interpreted using Kingery's liquid-phase sintering model. Particle rearrangement accounts for a significant proportion of the overall densification and is closely related to the amount and viscosity of the liquid present. The oxidation resistance of fabricated samples is good but, at temperatures above 1300° C, decreases with increasing alumina content in the starting mix. Modulus of rupture values of about 420 MPa at room temperature are high enough to encourage further work.

1. Introduction

Although the nitrogen ceramics that have generated the most interest for engineering applications are silicon nitride and the silicon nitride-based sialons, other potential candidates are silicon oxynitride [1] and its related O′-sialons. Early work at Newcastle [2] showed that the replacement

$$Si^{4+}N^{3-} \rightleftharpoons Al^{3+}O^{2-} \quad (1)$$

could occur in Si_2N_2O without change of structure although to a more limited extent than in β-Si_3N_4. The most recent determination [3] of the extent of solid solubility of alumina in silicon oxynitride

$$(2-x)Si_2N_2O + xAl_2O_3 \rightarrow 2Si_{2-x}Al_xO_{1+x}N_{2-x} \quad (2)$$

silicon oxynitride — alumina — O′-sialon

shows that the limit at 1800° C is 10 mol % Al_2O_3: 90 mol % Si_2N_2O; in the O′ general formula of Equation 2, $x \not> 0.2$.

The successful commercial development of β'-sialons [4, 5] uses yttria as a densifying additive to provide sufficient Y–Si–Al–O–N liquid at the processing temperature to allow pressureless sintering to theoretical density. Cooling gives β'-sialon with a grain-boundary glass which, by post-preparative heat-treatment, can be reacted with the matrix to give a slightly changed β' composition together with crystalline yttrium–aluminium garnet. For example:

$$\beta'\text{-}Si_5AlON_7 + \text{Y–Si–Al–O–N} \rightarrow \beta'\text{-}Si_{5+x}Al_{1-x}O_{1-x}N_{7+x} + Y_3Al_5O_{12} \quad (3)$$

sialon — glass — sialon — "YAG"

It was considered that similar methods might be used to produce O′-sialons, particularly because it is generally agreed (e.g. [6]) that the reaction

$$Si_3N_4 + SiO_2 \rightarrow 2Si_2N_2O \quad (4)$$

silicon nitride — silica — silicon oxynitride

does not occur in the solid state but requires a transient liquid, in which the reactants can dissolve and from which the product is precipitated. In a preliminary report [7] we have shown that the reaction and densification of mixed powders of Si_3N_4, SiO_2, Al_2O_3 and Y_2O_3 produce O′-sialon ceramics with an intergranular glass phase that can be devitrified by post-preparative heat-treatment. The present paper amplifies this earlier report and describes additional experimental work to confirm that O′-sialons show promise as engineering ceramics.

Yttria was selected as a densifying additive for three reasons. Firstly because, with alumina, it provides a suitable high-temperature Y–Si–Al–O–N liquid that is effective as a reaction medium for the formation of β'-sialons and also for their densification by liquid-phase sintering. Secondly because compatibility relationships in the Y–Si–Al–O–N system [8] show that yttrium disilicate, $Y_2Si_2O_7$, can coexist with silicon oxynitride and O′-sialon. Finally, multiphase ceramics based on silicon nitride with yttrium disilicate as a grain-boundary phase are reported [9] to have excellent oxidation resistance.

2. Experimental procedure

The raw materials were: (i) silicon nitride (Grade LC10, H.C. Starck, West Germany) with major impurities 3 wt % surface SiO_2, 0.02 wt % Fe_2O_3, 0.05 wt % Al_2O_3, 0.07 wt % CaO; (ii) crushed vitreous silica (Thermal Syndicate Ltd, England) of greater than 99.9% purity; (iii) alumina (Grade A16 Alcoa, America) 99.7% purity; and yttria (Rare Earth

*Present address: Division of Materials Science, CSIRO, Melbourne, Australia.

0022–2461/88 $03.00 + .12

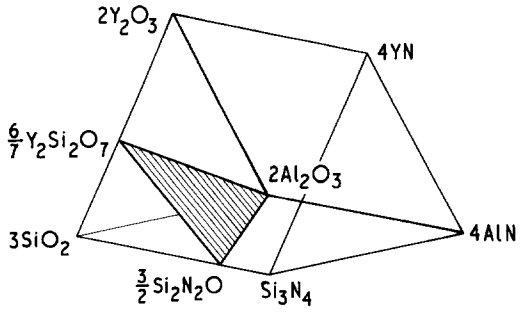

Figure 1 The Si_2N_2O–Al_2O_3–$Y_2Si_2O_7$ plane in the Y–Si–Al–O–N system.

Products Ltd, England), 99.5% purity. Mixed powders of Y_2O_3, SiO_2, Si_3N_4 and Al_2O_3 were ball-milled using high-density alumina media in isopropyl alcohol for 25 h. The resulting slurries were then continuously stirred on a hotplate to avoid segregation during the evaporation of alcohol, the last traces of which were removed by vacuum drying at 115° C. Both the surface silica on the silicon nitride and the alumina pick-up from the milling were taken into account in calculating compositions. All starting compositions are on the Si_2N_2O–Al_2O_3–$Y_2Si_2O_7$ sub-system plane of the Y–Si–Al–O–N system (see Fig. 1) and are given in Table I. The batch identification letter and numeral (e.g. A10) show the extent of aluminium substitution in the O′-sialon and the weight ratio $Y_2Si_2O_7$/O′-sialon, assuming these to be the only phases in the product. Compositions A, B and C have aluminium contents within the O′ solubility limit; D is approximately on the limit; and E exceeds the limit. The numerals (e.g. 10 and 15) represent weight ratios "YS/O" (0.10 and 0.15, respectively); see the sixth column, in Table I.

Powder mixes were uniaxially pressed into pellets in steel dies and then cold isostatically pressed at 200 MPa before firing in nitrogen for 1 h at 1700 or 1800° C; heating rates were about 60° C min^{-1} up to firing temperature. To minimise bloating, mixes with high aluminium contents (compositions D and E) required a modified two-stage firing cycle in which samples were held at an intermediate temperature, usually for 0.5 or 1 h at 1500 or 1600° C, before heating to the maximum temperature.

In all cases, samples were packed in a protective powder bed containing silica and silicon nitride in equimolar amounts. Weight losses were negligible, indicating no appreciable change from the starting composition, and all samples reached greater than 95% theoretical density by pressureless sintering.

To assist the devitrification of grain-boundary glass, samples were given a post-preparative heat-treatment for 25 h at 1300° C in nitrogen. However, subsequent work [10] has shown that even 100 h at 1300° C does not change the unit-cell dimensions of the first-formed O′-sialon and, although minor amounts of non-equilibrium mullite are observed, the devitrification of the Y–Si–Al–O–N glass is not complete.

2.1. Densification

The densification behaviour was determined using compositions with YS/O ratios of 0.15. Different samples were heated for 0.5 h each at successively higher temperatures at 100° C intervals in the range 1400 to 1800° C; see Curve (d) of Fig. 2. Unfired and fired bulk densities were obtained using mercury immersion and were compared with fully dense O′ materials of the same composition obtained by hot-pressing.

2.2. Oxidation resistance

Oxidation resistance was measured by heating at a rate of 3° C min^{-1} from 1000 to 1500° C in static air at one atmosphere and continuously recording the weight change on a microbalance.

2.3. Modulus of rupture

Modulus of rupture was measured at room temperature on bars 25 mm long × 5 mm wide × 3 mm high, ground on 800 mesh silicon carbide abrasive and lapped with 6 μm diamond paste. A three-point bend jig with silicon carbide knife edges and an outer span

TABLE I Composition of starting mixes

Batch	Composition (wt %)				YS/O†	Equivalent percentage				
	Y_2O_3	SiO_2	"Si_3N_4"*	Al_2O_3		Y	Si	Al	O	N
D5	2.8	25.3	61.5	10.4	0.05	1.0	90.9	8.1	32.8	67.2
A10	5.8	27.8	63.8	2.6	0.10	2.0	96.0	2.0	30.0	70.0
B10	5.6	27.2	62.4	4.8	0.10	2.0	94.2	3.8	31.3	68.7
C10	5.5	26.5	60.8	7.2	0.10	2.0	92.4	5.6	32.6	67.4
D10	5.4	25.8	59.2	9.7	0.10	1.9	90.4	7.7	34.1	65.9
E10	5.0	24.1	55.4	15.4	0.10	1.8	85.9	12.3	37.4	62.6
A15	8.5	28.2	61.1	2.2	0.15	3.0	95.3	1.7	31.6	68.4
B15	8.3	27.5	59.6	4.6	0.15	3.0	93.4	3.7	33.0	67.0
C15	8.1	27.0	58.4	6.4	0.15	2.9	91.9	5.1	34.0	66.0
D15	7.8	26.1	56.5	9.5	0.15	2.9	89.5	7.6	35.7	64.3
E15	7.4	24.6	53.3	14.6	0.15	2.7	85.4	11.9	38.7	61.2
A20	10.7	28.5	58.9	1.9	0.20	3.9	94.6	1.6	33.0	67.0
B20	10.4	27.9	57.7	4.0	0.20	3.8	93.0	3.2	34.1	65.9
C20	10.2	27.3	56.4	6.2	0.20	3.7	91.2	5.0	35.3	64.7
D20	9.9	26.4	54.6	9.2	0.20	3.6	88.7	7.5	37.0	63.0

*"Si_3N_4" includes 3 wt % surface SiO_2.
†YS/O represents the weight ratio $Y_2Si_2O_7$/O′-sialon.

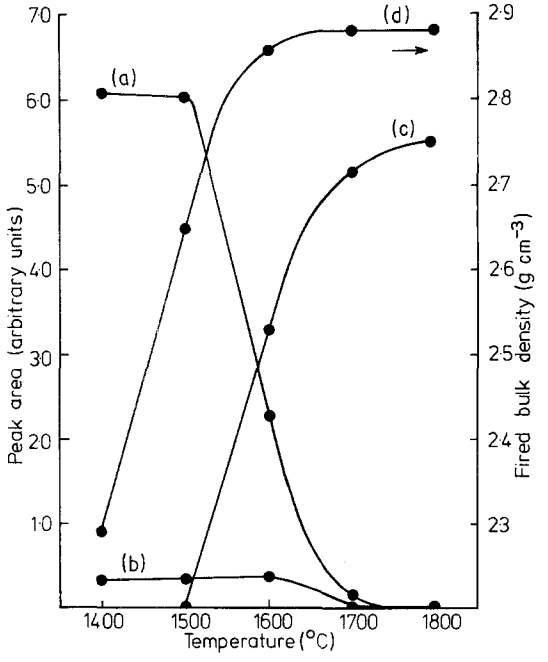

Figure 2 Densification and O′-sialon formation for samples of Batch C15, each after 0.5 h at one temperature in the range 1400 to 1800° C. X-ray diffraction peak heights: (a) α-Si_3N_4, (b) β-Si_3N_4, (c) O′-sialon. Product density is given by (d).

of 19 mm was used in an Instron test machine with a crosshead speed of 0.01 cm min^{-1}.

2.4. Phase identification

All reaction, devitrification and oxidation products were identified and phase changes were followed using Cu$K\alpha$ X-ray powder diffraction either with a Hägg–Guinier focusing camera or with a diffractometer. Unit-cell dimensions of phases were determined from powdered products in a 114 mm diameter Philips camera with filtered Cr$K\alpha$ radiation using Nelson–Riley extrapolation.

3. Results and discussion

3.1. Densification

In the mixes used, the oxide concentration varies from about 35 to nearly 50% of the total weight and, from the ternary oxide equilibrium diagram [11], a high proportion of this will form liquid at temperatures of 1500° C and above. Significant densification might therefore be anticipated by particle rearrangement. The formation and densification of O′-sialons is expected to be similar to that of β'-sialon and of silicon nitride, where the densification mechanism and kinetics have been interpreted by Hampshire and Jack [12] in terms of Kingery's model [13] for liquid-phase sintering. Here, the successive stages are:

(i) particle rearrangement where the rate and extent of shrinkage depend upon the volume and viscosity of liquid;

(ii) solution–precipitation, in which

$$\Delta V/V_0 \propto t^{1/n} \quad (5)$$

where V_0 is the initial volume and ΔV the change in volume after time t for prismatic particles. If solution into or precipitation from the liquid is rate-controlling, $n = 3$, and if the slowest step is diffusion through the liquid, $n = 5$;

(iii) solid–solid interaction where liquid-phase sintering effectively ceases.

The typical progress of densification and the subsequent formation of an O′-sialon is shown in Fig. 2 for Batch C15. Densification starts and is half complete before the formation of any O′-sialon. This initial period corresponds to the rearrangement Stage (i) in which the shrinkage is due to the presence of relatively large amounts of liquid. As might be expected, the densification rate increases with aluminium concentration and hence increasing volume of liquid. The liquid contains dissolved silicon nitride, i.e. it is an oxynitride, and during Stage (ii) silicon, aluminium, oxygen and nitrogen are removed from the liquid and precipitated as O′-sialon. At intermediate temperatures (1450 to 1600° C) the precipitation of O′ is slow and the amount of transient liquid decreases very slowly, thus allowing a maximum proportion of densification by particle rearrangement. At higher temperatures precipitation of O′ is rapid and is completed with depletion of liquid after a short time. Limited observations suggest that the solution–precipitation Stage (ii) is diffusion-controlled as in the densification of silicon nitride with yttria [12]. At low temperatures in the Y_2O_3–Si_3N_4 system the low liquid content and its high viscosity limit the amount of particle rearrangement and this, together with the slow rate of solution–precipitation in Stage (ii), gives low final densities.

By contrast, the large amount of liquid formation in the present system gives high densities even though the rate of Stage (ii) is probably equally slow. Indeed, for compositions that are difficult to densify, e.g. those with low aluminium concentrations, a modified firing cycle to prolong the rearrangement stage and maximize the amount of liquid gives higher final densities. Samples are fired in two stages with an intermediate temperature hold instead of a single-stage firing. For example, a specimen of Batch A15 had a density of 2800 kg m^{-3} after single-stage firing for 1 h at 1800° C. With two stages, 1 h at 1600° C followed by 1 h at 1800° C, the density was 2860 kg m^{-3}, an increase of more than 2%.

3.2. Effect of aluminium concentration

As previously stated, the overall densification in the present O′-sialon system depends largely on particle rearrangement which, in turn, depends on the amount and viscosity of the liquid. In yttria-densified β'-sialon the electron probe microanalysis of grain-boundary glass in three different samples [14] gives very similar compositions within the range

$$Y_{9-11}Si_{12-14}Al_{14-17}O_{57-58}N_{4-5}$$

If it is assumed that the liquid composition in the present system is not too different from that of this glass, then the amount of liquid will increase as the overall composition of the mix approaches that of the glass. In the different batches (Table I) the amount of liquid will thus increase from A to D. Fig. 3, for

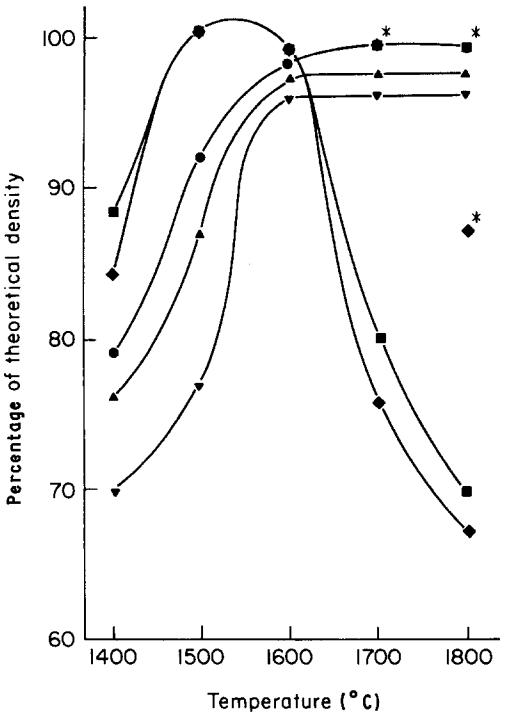

Figure 3 The effect of alumina content on density after 0.5 h at temperature for batches with YS/O ratio 0.15 (for definition see Table I): (▼) A15, (▲) B15, (●) C15, (■) D15, (◆) E15. Asterisks indicate the modified cycle (for explanation see text).

batches with YS/O = 0.15, shows that the densification rate and the final density, at least to 1600° C, increase as expected.

Densities apparently greater than theoretical are obtained for Batches D15 and E15 at 1500° C, but at this temperature the samples contained significant amounts of unreacted α-Si_3N_4 the density of which is 15% higher than that of O′-sialon. With single-stage firing, the densities of both materials then decrease markedly at firing temperatures above 1600° C due to the volatilization of silicon monoxide and nitrogen with consequent bloating and formation of β'-sialon. It is thought that rapid heating to 1600° C and above does not allow the formation of stable oxynitride liquids; the dissolution of silicon nitride is perhaps incomplete. A two-stage firing with a long intermediate-temperature soak minimizes the bloating and the formation of β'-sialon.

3.3 Effect of YS/O ratio

For any given alumina addition, Fig. 4 shows that increasing the YS/O ratio increases the rate of densification. If the liquid composition is that given in Section 3.2., then for the batches examined in the present work the overall composition will approach more closely that of the liquid as the YS/O ratio increases and so the amount of liquid will increase. The densification behaviour is again explicable.

3.4. Oxidation resistance

The continuous weight gain by heating from 1000 to 1500° C in air at 3° C min^{-1} is shown for Batches A15 to E15 in Fig. 5. Up to 1150° C the oxidation behaviours of all five compositions are similar and show only very small weight changes. At higher temperatures the oxidation resistance decreases with increasing aluminium content and above ~ 1350° C the oxidation rate increases rapidly. The solidus temperature in the Y_2O_3–Al_2O_3–SiO_2 system is at 1350° C and so in an oxidizing environment any Y–Si–Al–O–N composition will eventually give a liquid component in the oxidized layer. From the ternary oxide equilibrium diagram and for the compositions of the present work, the volume of liquid will increase with increasing alumina concentration. Impurities are also expected to depress the solidus temperature, increase the volume of liquid, and hence decrease the oxidation resistance.

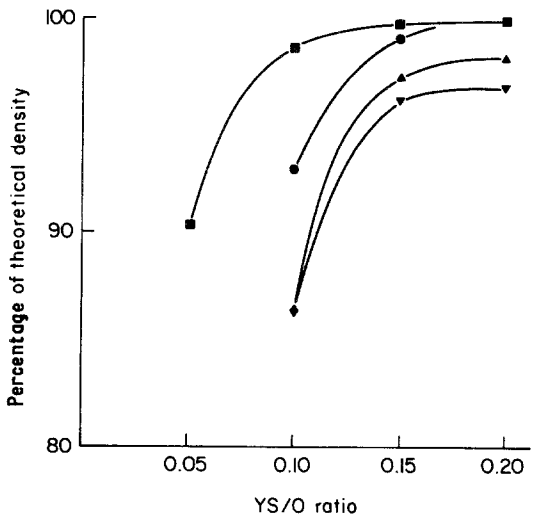

Figure 4 Effect of YS/O ratio (for definition see Table I) on density after 1 h at 1700° C for different compositions: (▼) A, (▲) B, (●) C, (■) D.

Fig. 6 shows scanning electron micrographs of the oxidized layer–O′ interface for compositions A15 to E15 after 0.5 h in air at 1500° C. The oxide layer thickness increases with aluminium concentration in accordance with the weight gain, and the porosity of the oxide also increases as a result of the increasing liquid volume. The inner layer of oxide appears to be more highly porous, presumably because of nitrogen

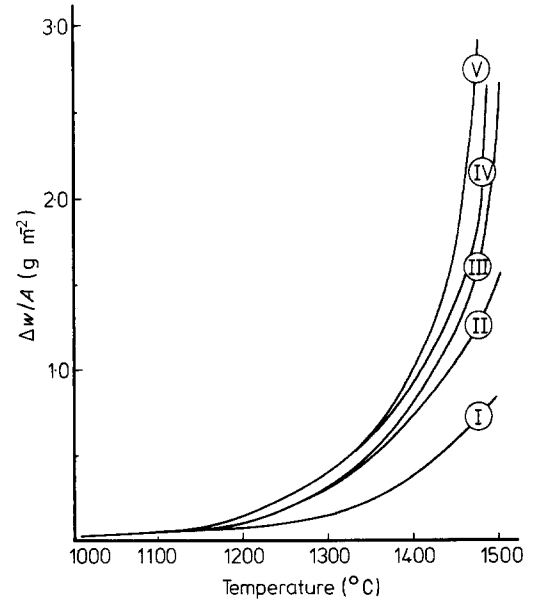

Figure 5 Oxidation behaviour on heating from 1000° C to the indicated temperature at 3° C min^{-1} for densified O′-sialons: (I) A15, (II) B15, (III) C15, (IV) D15, (V) E15.

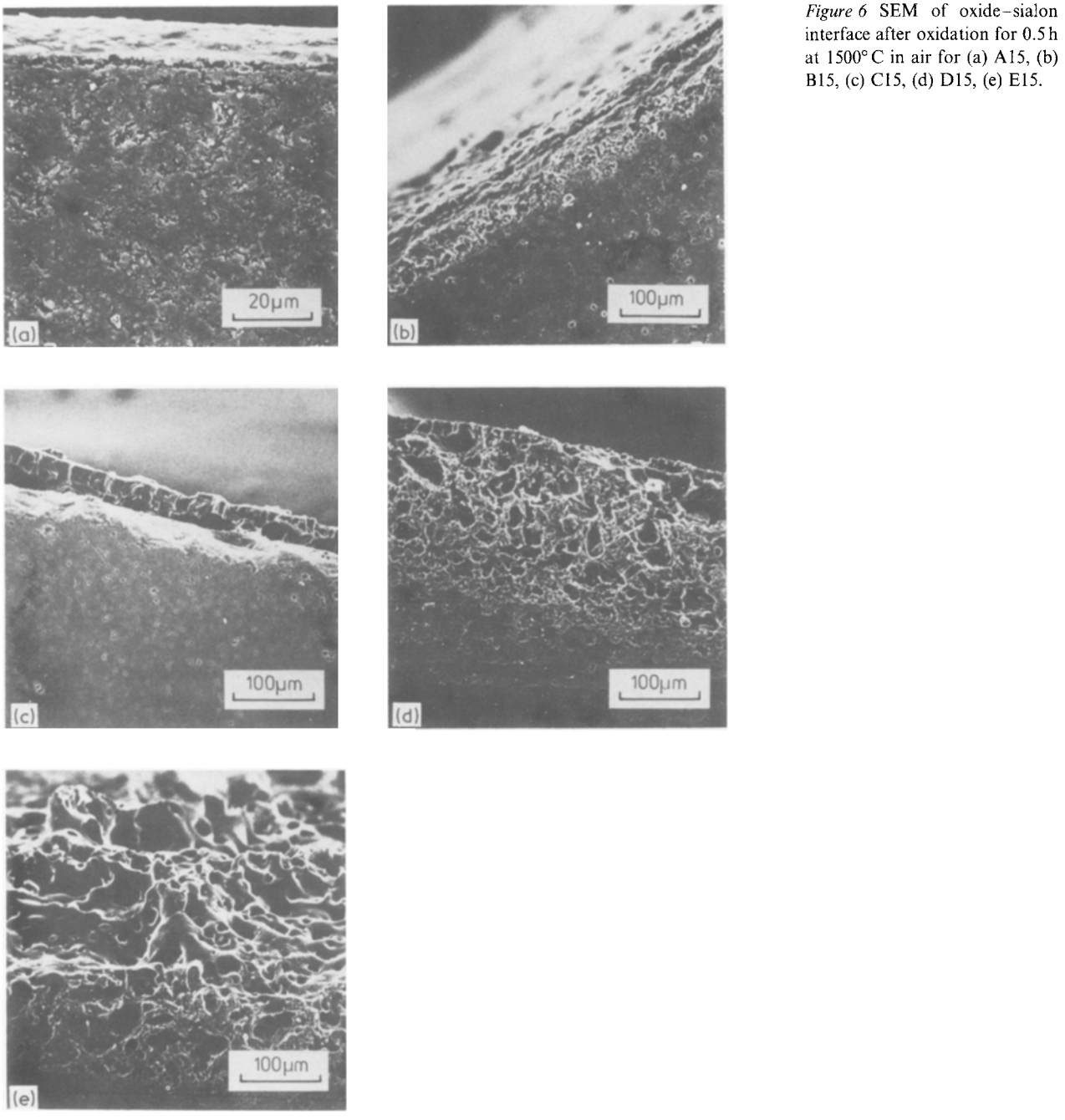

Figure 6 SEM of oxide–sialon interface after oxidation for 0.5 h at 1500° C in air for (a) A15, (b) B15, (c) C15, (d) D15, (e) E15.

evolution. For Batch E15 the pores interconnect the surface with the O′ interface and so accounts for the very fast oxidation rate.

In Fig. 7 scanning electron micrographs of the surfaces of oxidized samples B15 to E15 show extensive microcracking due to the $\beta \rightarrow \alpha$ transformation of the cristobalite that is formed as the major crystalline phase. In A15, O′ and $Y_2Si_2O_7$ are the major surface phases and cristobalite only a minor one; the absence of micro-cracks is therefore explained.

3.5. Strength measurements

Modulus of rupture measurements for the A15 to E15 series are summarized in Table II and suggest that the strength increases with density (A15 to D15). The differences, however, are hardly significant. The values themselves, although not remarkable (~ 420 MPa), are sufficiently high for pressureless-sintered materials at an early stage of development to suggest that improvements in powder processing and fabrication might bring O′-sialons into the same range as β'-sialons and hot-pressed silicon nitride. Scanning electron micrographs of the fracture surfaces of A15 to C15 show porosity with an average pore size of 5 μm, i.e. much greater than the grain size of the ceramic (Fig. 8a). For D15 and E15 the pore size is much smaller ($\sim 0.5\,\mu$m) but the pores are interconnected over regions of $\sim 20\,\mu$m (Fig. 8b). Both kinds of defect will limit the strength of the material and

TABLE II Modulus of rupture for selected O′-sialons

Batch	Density ($kg\,m^{-3}$)	Modulus of rupture (MPa)
A15	2790	350
B15	2830	410
C15	2880	430
D15	2900	440
E15	2900	440

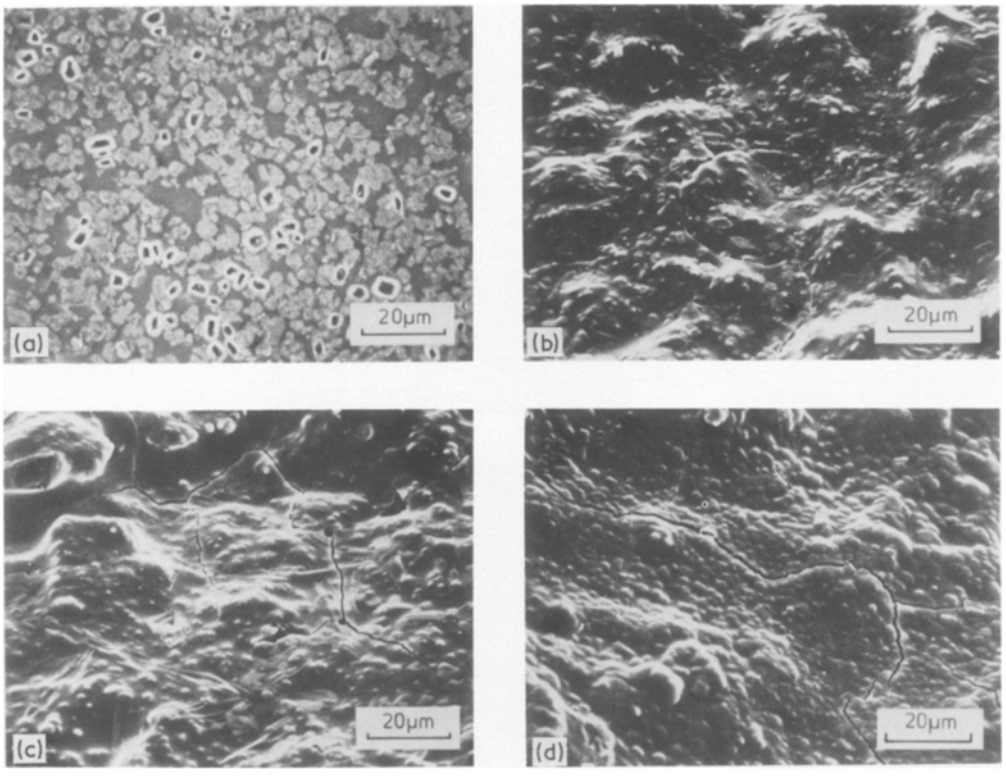

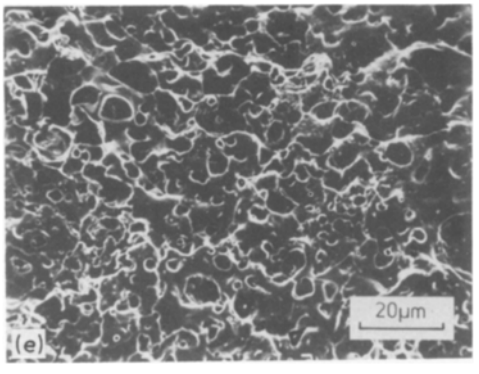

Figure 7 SEM of oxidized surface after 0.5 h at 1500° C in air for (a) A15, (b) B15, (c) C15, (d) D15, (e) E15.

support the suggestion that improved processing will give better properties.

4. Conclusions

High-density O′-sialon ceramics can be fabricated by pressureless sintering in nitrogen with yttria as a densifying additive. Post-preparative heat-treatment to devitrify the intergranular glass gives yttrium disilicate as the main grain-boundary phase.

Densification is described by Kingery's model for liquid-phase sintering and depends markedly on the amount and the viscosity of the liquid. Particle rearrangement, which accounts for more than half of the densification, occurs prior to the formation of O′-sialon by a solution–precipitation process. Adequate time for particle rearrangement, and hence higher final density, is most readily achieved by a two-stage firing sequence in which the specimen is held at an intermediate temperature. The two-stage firing also reduces the bloating that occurs in the single-stage firing of compositions with high alumina contents.

Increasing additions of alumina, and of yttria with excess silica to give yttrium disilicate, both facilitate densification by increasing the volume of transient liquid.

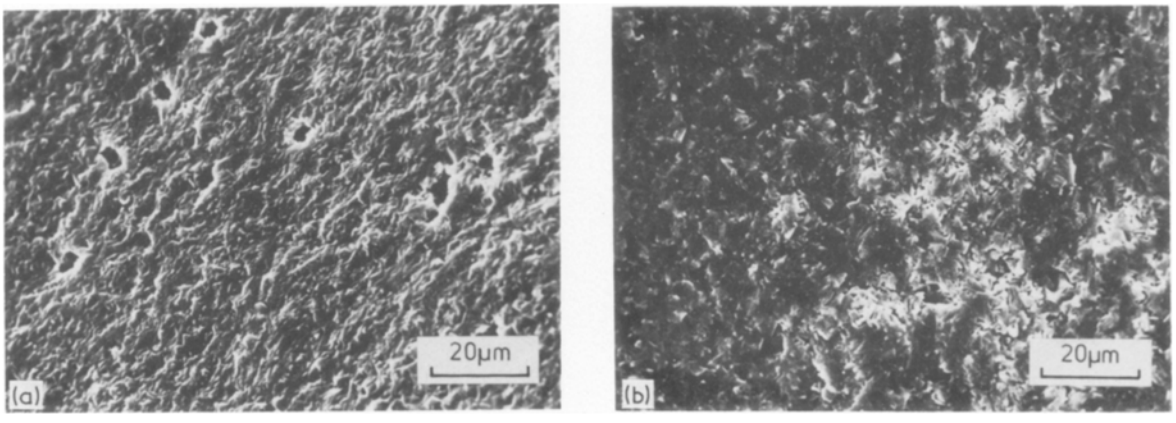

Figure 8 SEM of modulus-of-rupture fracture surfaces: (a) C15, pore size $\sim 5\,\mu m$; (b) E15, 20 μm regions of interconnected small pores (pore size $\sim 0.5\,\mu m$).

Increasing alumina decreases the oxidation resistance of fully densified O′-sialons, especially above 1350° C. Finally, the strengths of fabricated samples are not remarkably high but suggest that further process development will bring them into the same range as the other dense nitrogen ceramics currently used in engineering applications.

Acknowledgements

We thank the Wolfson Foundation for a postdoctoral research associateship to M.B.T. and the Leverhulme Trust for an emeritus fellowship to K.H.J.

References

1. M. E. WASHBURN, *Amer. Ceram. Soc. Bull.* **46** (1967) 667.
2. K. H. JACK, *Trans. J. Br. Ceram. Soc.* **72** (1973) 376.
3. M. B. TRIGG and K. H. JACK, *J. Mater. Sci. Lett.* **6** (1987) 407.
4. K. H. JACK, *Sci. Ceram.* **11** (1981) 125.
5. R. J. LUMBY, E. B. BUTLER and M. H. LEWIS, in "Progress in Nitrogen Ceramics", edited by F. L. Riley (Nijhoff, The Hague, 1983) p. 683.
6. Z. K. HUANG, P. GREIL and G. PETZOW, *Ceram. Int.* **10** (1984) 14.
7. M. B. TRIGG and K. H. JACK, In "Ceramic Components for Engine", edited by S. Sōmiya, E. Kanai and K. Ando (KTK Scientific Publishers, Tokyo, 1984) p. 199.
8. I. K. NAIK and T. Y. TIEN, *J. Amer. Ceram. Soc.* **62** (1979) 642.
9. F. F. LANGE, S. C. SINGHAL and R. C. KUZNICKI, *ibid.* **60** (1977) 249.
10. M. B. TRIGG, *Rev. Chim. Min.* **22** (1985) 449.
11. I. A. BONDAR and F. Ya. GALAKHOV, in "Phase Diagrams for Ceramics, 1969 Supplement", edited by E. M. Levin, C. R. Robbins and M. F. McMurdie (American Ceramic Society, Columbus, 1969) Fig. 2586, p. 165.
12. S. HAMPSHIRE and K. H. JACK, *Proc. Br. Ceram. Soc.* **31** (1981) 37.
13. W. D. KINGERY, *J. Appl. Phys.* **30** (1959) 301.
14. K. H. JACK, "The Role of Additives in the Densification of Nitrogen Ceramics"; Final Technical Report to the European Research Office, US Army Grant No. DAERO-76-G-067 (1977).

Received 30 October 1986
and accepted 28 January 1987